Journal of Catalysis **182,** 497–506 (1999)
Article ID jcat.1998.2373, available online at http://www.idealibrary.com on IDEAL®

A Transient Kinetic Study of the Mechanism of the $NO/C_3H_6/O_2$ Reaction over $Pt–SiO_2$ Catalysts

Part 2: Steady-State Isotopic Transient Kinetic Analysis

R. Burch, A. A. Shestov,[1] and J. A. Sullivan

Catalysis Research Centre, Chemistry Department, University of Reading, Whiteknights, Berkshire, RG6 6AD, United Kingdom

Received September 11, 1998; revised December 3, 1998; accepted December 3, 1998

Steady-state isotopic transient kinetic analysis (SSITKA) of the $NO/C_3H_6/O_2$ reaction, using $^{14}NO \rightarrow {}^{15}NO$ switches, has been carried out over a 1% $Pt–SiO_2$ catalyst at four different temperatures. The results indicate that below the temperature of the maximum NO_x conversion there are no NO adsorption/desorption processes taking place under these steady-state conditions. Moreover, less than 15% of the catalyst surface is covered with N_2 or N_2O precursors. N_2O is the "isotopically first" product while N_2 is the second. The surface lifetime of N_2O precursors is relatively short while the surface lifetime of N_2 precursors is significantly longer. The production of N_2 and N_2O are both increased by raising the temperature. In the case of N_2O, this seems to be solely due to an increase in the concentration of active sites on the catalyst while in the case of N_2 the increase in the number of active sites is accompanied by an increase in their intrinsic activity. At temperatures above the maximum in the NO_x conversion there is a discernible amount of NO desorption taking place under steady-state conditions. This is rationalised by the formation of $NO_{2\,(ads)}$ species on the now-oxidised Pt surface. The SSITKA results are found to support the previously proposed reaction mechanism for the $NO/C_3H_6/O_2$ reaction over Pt-based catalysts. Finally, a general form for the calculation of concentrations of adsorbed species from any SSITK analysis is presented.

Key Words: **Pt catalysts; lean-burn conditions; NO_x reduction; reaction mechanisms; SSITKA.**

INTRODUCTION

The reduction of NO_x under lean-burn conditions over Pt-based catalysts has been the focus of much recent interest in the literature (1–12). Detailed kinetic measurements from our laboratory have demonstrated that two different reaction mechanisms operate over these catalysts, the controlling mechanism depending of the type of hydrocarbon used (7, 8). These mechanisms can be divided into situations where the reducing agents are strongly adsorbed (C_2H_4, C_3H_6, $C_6H_5CH_3$) or alternatively where they are weakly adsorbed (C_2H_6, C_3H_8,). In the former conditions, the Pt surface (below the temperature of maximum NO_x conversion) is reduced (metallic) and predominantly covered in carbonaceous species. The O_2 reacts to remove these carbonaceous species and the deNO_x reaction takes place through the dissociation of NO on vacant Pt sites (7). Under the latter conditions, the reaction proceeds through an NO_2 intermediate. In this case the Pt surface is predominantly covered in adsorbed oxygen, NO is oxidised to NO_2 on the metal and moves to the support, or the metal support interface, where it interacts with, and is reduced by, the hydrocarbon (8). Some hydrocarbons may follow both types of reaction mechanism, depending upon the precise reaction conditions. Thus, C_8H_{18} has been found to mimic both C_3H_6 and C_3H_8 over $Pt–Al_2O_3$ (13–14).

In Part I (29) we have presented results from a non-steady-state kinetic analysis which provide further evidence that the surface of the Pt changes as the reaction temperature is scanned through the range where the NO_x conversion reaches a maximum. The results are consistent with the previously proposed mechanism (7, 8) which concluded that at low temperatures the NO decomposes on a reduced Pt state, while at high temperatures the NO oxidises to NO_2 which may react on the support or at the metal–support interface.

Steady-state isotope transient kinetic analysis (SSITKA) (15–17) has previously been used in attempts to clarify the mechanisms of several reaction types, e.g., Fischer–Tropsch synthesis (18), CO hydrogenation (19), oxidative coupling of CH_4 (OCM) (20), and methanol synthesis (21). Generally the reactions which provide the clearest information are those where the surface contains large reservoirs of adsorbed intermediates which are slowly transformed to products. A SSITK analysis of the CO oxidation and CO/NO reactions over TWC-type materials has been published (22) while some attention, with regard to this technique, has also

[1] On leave from Boreskov Institute of Catalysis, RAS, Pr. Akademika Lavrentieva, 5, Novosibirsk, 630090, Russia.

0021-9517/99 $30.00

been paid to reactions designed to eliminate NO_x under oxidising conditions. Efstathiou *et al.* (23) and Janssen *et al.* (24, 25) have studied the $NO/NH_3/O_2$ reaction over V_2O_5–TiO_2 catalysts. Ozkan *et al.* (26, 27) have also studied the $NO/CH_4/O_2$ reaction over Pd–TiO_2 catalysts. In the present work, transient isotope techniques are used to obtain further information about the nature of the Pt surface under steady-state reaction conditions in the presence of strongly reducing hydrocarbons such as C_3H_6.

EXPERIMENTAL

In order to be able to reduce effects caused by interaction between the metal and the support, and discount reactions on the support itself, Pt–SiO_2 catalysts are used throughout this study. (It is known that Al_2O_3 supports can adsorb and desorb NO_x-type species at the temperatures used in our work (28)). The catalyst was prepared using incipient wetness impregnation of the required mass of a Pt(DNDA) solution (2.28% Pt) (DNDA = Di Nitro Di Amine) (Johnson Matthey) onto a pre-washed and dried sample of Grace SiO_2 with a grain size of 250–600 μm. The sample was dried at 110°C for 1 h and calcined in air at 500°C for 14 h. Surface areas and metal particle size measurements were performed on a home-made chemisorption apparatus. The Pt–SiO_2 had a total surface area of 280 $m^2\ g^{-1}$ and a metal dispersion of 22%.

Steady-State Isotopic Transient Kinetic Analysis of the $NO/C_3H_6/O_2$ Reaction

Due to difficulties balancing the pressure of the switch when low flows of NO are used the reaction was carried out under the following conditions: 1.63% NO, 8900 ppm C_3H_6, 8.8% O_2 in a total flow of 111 $cm^3\ min^{-1}$. 100 mg of catalyst (1% Pt–SiO_2) was used and the reactor was configured to minimise the dead volume prior to the catalyst. The NO is flowed from a cylinder of 95% NO in Ar. The Ar is used as an internal marker for the transient switch. The switch itself involved the removal of the ^{14}NO/Ar mixture and its replacement with a stream of ^{15}NO flowing at the same rate and adjusted to the same pressure using the two pressure transducers and a fine needle valve.

Such switches, which were performed at temperatures above and below the maximum in the NO_x conversion versus temperature curve, change the concentration of NO which reaches the catalyst by 5%. Thus, the mixture changes from being 1.63% ^{14}NO, 0.89% C_3H_6, 0.08% Ar and 8.79% O_2 to being 1.81% ^{15}NO, 0.89% C_3H_6 and 8.79% O_2. The N-containing products of the reaction, i.e., N_2, N_2O, and NO_2 and their isotopically labelled analogues, were monitored by mass spectrometry as a function of time after each switch.

The catalyst was pretreated in the reaction mixture at 450°C for 1 h prior to being cooled to the required temperature in the reactant flow. The sample was then held in the reactant flow for 30 min at this temperature to ensure steady state reaction. The system was left in the flow of ^{15}NO for up to 5 min after the switch and then the reverse switch ($^{15}NO \rightarrow {}^{14}NO$) was performed.

Usually these profiles are presented as showing one species decreasing (in this case m/e = 28 as N_2 formation ceases), another species increasing (in this case m/e = 30 as $^{15}N_2$ formation begins and rises to steady state), and a third species rising from zero to go through a maximum before again decreasing to zero (in this case the mixed $^{15}N^{14}N$ species at m/e = 29). However, in this specific case the $^{15}N_2$ formation cannot be analysed because this peak overlaps with ^{14}NO. The normalised responses of the three products should add up to 1, however, and thus the profile for the $^{15}N_2$ can be deduced. The increasing m/e = 28 data (due to $^{14}N_2$) for the second switch, i.e., when ^{14}NO is switched back into the reactant stream, can also be used to simulate the profile which would be expected for the $^{15}N_2$ species during the original $NO \rightarrow {}^{15}NO$ switch. Both these treatments assume that the reaction remains at steady state throughout the course of the switch and is not affected by the change in NO concentration. The latter treatment also assumes that 5 min in the ^{15}NO reactant mixture is enough time to fully remove the ^{14}N species from the catalyst surface and the surrounding gas phase, thereby allowing the reverse switch to be directly compared to the original switch.

A similar procedure had to be adopted with the N_2O profiles due to the large CO_2 peak seen at m/e = 44. In this case the m/e = 45 and 46 peaks are monitored.

The percentage conversions of reactant from NO into N_2 and N_2O are calculated from observed mass spectrometer partial pressures and calibration plots of ppm versus partial pressure.

The N_2 and N_2O figures for the τ value (the mean surface residence time) are obtained by calculating the difference in area under the Ar, N_2, and N_2O normalised profiles and adding half the area of the mixed labelled species, $^{14}N^{15}N$ or $^{14}N^{15}NO$ (as half of this area = τ ^{14}N leading to the mixed product). The NO and NO_2 values can be calculated directly and all the NO calculations take the NO_2 fragment at mass 30 into account before τ values are calculated.

RESULTS

The results in Part 1 (29) show the general product versus temperature profile for the $NO/C_3H_8/O_2$ reaction. However, as discussed in the experimental section, the reaction conditions for the study of $^{14}NO \rightarrow {}^{15}NO$ switches involve significantly higher NO concentrations than those used in the previous studies of the $NO/C_3H_6/O_2$ reaction and the transient reactions mentioned previously (29). These are necessary to obtain acceptable signal-to-noise ratios and properly pressure balanced flows. This results in an increased NO_2 formation in the gas phase: the gas phase

production of NO_2 is second order in NO. It also causes the temperature for the maximum NO_x conversion to increase to ca. 275°C because the rate of combustion of C_3H_6 is inhibited by NO (12). Therefore, $^{14}NO \rightarrow {}^{15}NO$ switches were carried out over the 1% Pt–SiO_2 catalysts at temperatures of 225, 247, and 263°C (below the temperature of maximum NO_x conversion), and at 328°C which was above the maximum. At the first three temperatures here the reactor is operating in a differential manner while in the last case this is obviously not so as conversion of C_3H_6 is at 100%.

Generally speaking the information which can be gleaned from these SSITK experiments includes:

- The total concentration of all adsorbed labelled species;
- The concentration of surface sites generating products;
- The reversibility of reactant adsorption;
- The average lifetimes of the intermediate species on the catalyst surface which lead to product molecules;
- The order of isotopic production of product molecules;

Further analysis of the observed profiles using numerical methods in conjunction with mathematical modelling can yield detailed kinetic information regarding the mechanism of the reaction. Such an analysis would determine the nature of adsorbed intermediates and quantitative values of such parameters as surface rates and the number and concentration of surface intermediates. This mathematical treatment of the profiles is beyond the scope of the present paper and will be dealt with in a subsequent publication (30).

Under the reaction conditions used, which were chosen to minimise the pressure change seen during the switch of ^{14}NO for ^{15}NO, an amount of NO_2 was generated. However, as discussed above, experiments over SiO_2 and in empty quartz reactors have shown that this is formed from the gas phase interaction of NO and O_2 and not from interactions with the catalyst. Switches of gas in the empty reactor and over the SiO_2 have also shown that this NO_2 is delayed in its removal from the reactor relative to NO and argon. Thus, in calculating parameters from the NO_2 profiles, a profile relating to a switch of ^{14}NO for ^{15}NO through an empty reactor is taken as a reference profile.

Figure 1 shows the ^{15}NO profiles obtained when ^{15}NO replaces ^{14}NO in the reactant stream. The profile for ^{15}NO rather than that for ^{14}NO is monitored as the former does not suffer from any overlaps with other molecules, while the latter shares a common molecular mass with $^{15}N_2$. Four profiles are shown. First is the profile found for ^{15}NO over SiO_2 from the switch $^{14}NO/C_3H_6/O_2 \rightarrow {}^{15}NO/C_3H_6/O_2$, at room temperature, then two profiles referring to the same gas switch at different reaction temperatures over the 1% Pt–SiO_2 catalyst, and finally an inverted Ar trace.

It can be seen that there are no NO desorption processes taking place on the surface under steady-state reaction conditions. If such processes were occurring then there would be a difference between the inverted Ar profile and the ^{15}NO profile. This was the not case for SiO_2 or for the 1% Pt–SiO_2 catalyst at 263°C. Identical ^{15}NO profiles were obtained at 247 and 225°C (results not reproduced here). However, Fig. 1 shows that the ^{15}NO profile from the $^{14}NO/C_3H_6/O_2 \rightarrow {}^{15}NO/C_3H_6/O_2$ switch over the 1% Pt–SiO_2 catalyst at 328°C exhibits a relatively large difference between the ^{15}NO profile and that of the Ar. The ^{15}NO signal initially rises sharply but only to ca. 90% of its maximum value, to which it then increases slowly over about 30 s.

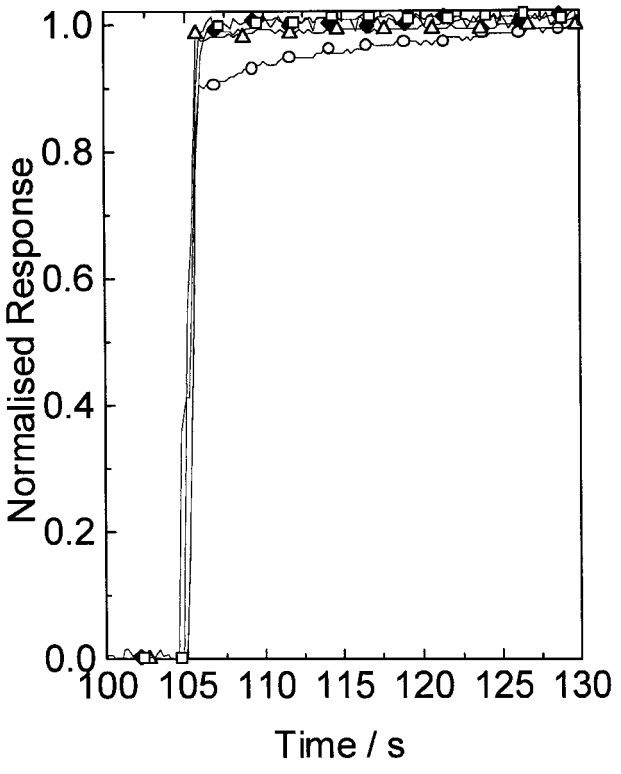

FIG. 1. Comparison of ^{15}NO traces seen following the $^{14}NO/C_3H_6/O_2 \rightarrow {}^{15}NO/C_3H_6/O_2$ switch over SiO_2 (Δ) at room temperature and over a 1% Pt–SiO_2 catalysts at 263°C (□) and at 328°C (○). A profile for the inverted normalised Ar trace is also shown (◆).

In general the NO_2 profiles are rather noisy (results not shown) except in the case where the switch is carried out at 328°C where a lot of NO_2 is produced. However, to a first approximation there is no difference between the NO_2 profiles obtained with the catalyst or when an empty reactor or SiO_2 alone is used. Thus, within the limits of our experiment, there is no NO_2 desorption from the catalyst surface under steady-state reaction conditions.

Figure 2 shows a typical product response from the NO to ^{15}NO switch. It can be seen that the doubly unlabelled N_2 and N_2O species decrease rapidly after the switch and that only a relatively small amount of such species are formed after the NO is removed from the stream. Generally speaking

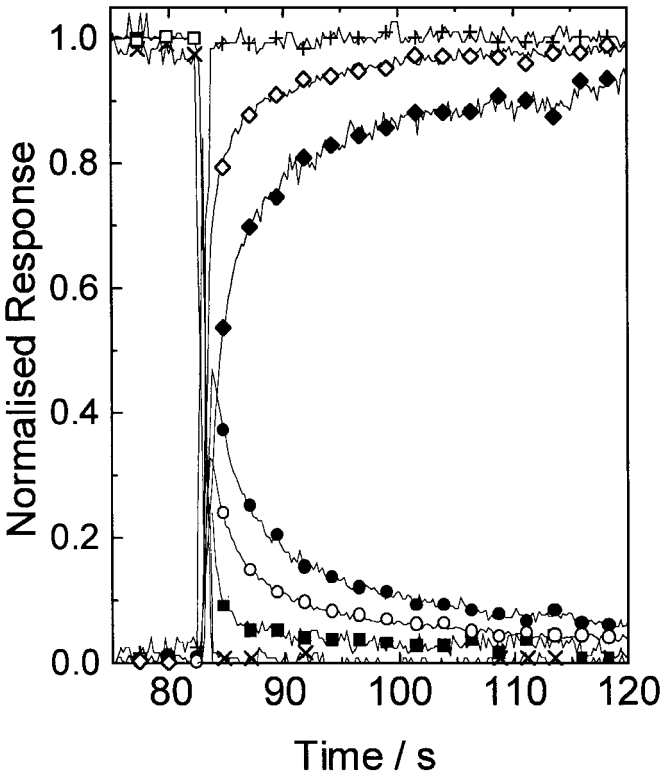

FIG. 2. Typical product profiles seen when ^{14}NO is replaced by ^{15}NO in the $NO/C_3H_6/O_2$ reaction over 1% $Pt–SiO_2$. Feed: 1.63% NO, 8900 ppm C_3H_6, 8.8% O_2, T = 225°C. ■, $^{14}N_2$; ●, $^{14}N^{15}N$; ◆, $^{15}N_2$; ×, Ar; +, Inv. Ar; □, $^{14}N_2O$; ○, $^{14}N^{15}NO$; ◇, $^{15}N_2O$.

doubly unlabelled N_2O desorbs from the catalyst within the time-scale of the switch. A mixed N_2O signal is also observed indicating that there is a reservoir of intermediate species on the surface which can make N_2O and which remain on the catalyst after the ^{14}NO is removed.

The doubly unlabelled N_2 species also decreases very quickly once the ^{14}NO is replaced by ^{15}NO, but there is a difference between this profile and that seen for Ar. This indicates that the surface can continue making $^{14}N_2$ for a short period of time after the ^{14}NO is removed. A mixed N_2 signal is also seen and this, as does the mixed N_2O signal, passes through a maximum before slowly decreasing to zero, again indicating the presence of a reservoir of N_2 precursors which remain on the catalyst surface for some time after the switch.

Finally, the fully doubly labelled products $^{15}N_2$ and $^{15}N_2O$ are observed. These normally reach steady state at times up to 3 min after the switch, i.e., once the signal for the mixed product has returned to a value of zero.

It should be recalled that one profile from each set of products is generated mathematically using the fact that the sum of all the normalised profiles of each product is 1. In the case of the N_2 profiles this is the m/e = 30 profile representing $^{15}N_2$ while in the case of the N_2O profiles it is the m/e = 44 representing the $^{14}N_2O$. As discussed in the Experimental section this is because of the overlaps seen at these masses with ^{14}NO and CO_2. The reason why the difference in the m/e = 44 peak cannot be used is because there is far more CO_2 formed than N_2O and therefore the normalised profile for the change in m/e = 44 is usually quite noisy. However, to a first approximation it does follow the same trend as the generated N_2O profile.

Another reason to feel confident about these arithmetically generated profiles comes from the reverse switches. In these cases, switches were carried out from ^{15}NO to ^{14}NO after the catalysts had been left in an $^{15}NO/O_2/C_3H_6$ stream for up to 5 min. It was observed (results not shown) that profiles for the increase of $^{14}N_2$ and the decrease of $^{15}N_2O$ mirrored very closely those calculated for the $^{15}N_2$ and $^{14}N_2O$ in the forward switch. Therefore, we are confident that the profiles generated arithmetically for the $^{15}N_2$ and the $^{14}N_2O$ are reliable.

As the reaction temperature is increased the percentage conversion of NO to N_2 and N_2O increases to a maximum. However, at temperatures above the maximum for deNO_x activity there is a far larger amount of NO_2 and it is difficult to get reproducible data for the $^{15}N_2O$ as well as the $^{14}N_2O$ profiles. This is because the $^{14}NO_2$ and the $^{15}N_2O$ species both have the same mass. This can be accounted for in the lower temperature reactions by using a calculated $^{14}NO_2$ profile and removing it from the emerging $^{15}N_2O$ profile. The $^{14}NO_2$ profile is calculated assuming that it is the inverse of the measured $^{15}NO_2$ profile. There is little error associated with doing this at lower temperatures where the NO_2 concentration is relatively small. However, this is not the case at temperatures above the NO_x conversion maximum.

The mean surface residence time for these various species can be evaluated from the difference between the normalised product traces and the normalised Ar (or inverse Ar) trace. The concentration of surface sites leading to these species can be evaluated using the residence times and the measured rates of reaction. The rates of reaction are calculated by using the changes recorded in the mass spectrometer profiles and a set of partial pressure versus mass spectrometer response plots.

The τ values for the doubly unlabelled species are calculated from the difference in area under the decreasing Ar curve and the decreasing signal representing the unlabelled compound. The mixed-labelled τ values are calculated directly from the area of the normalised mixed peak corresponding to $^{14}N^{15}N$ and $^{14}N^{15}NO$ multiplied by 0.5 (as only half the N_2/N_2O in the mixed-labelled species is ^{14}N).

The total mean surface residence time for the adsorbed species leading to N_2 (or N_2O) formation is calculated by adding the τ value calculated for the doubly unlabelled product to 0.5 times the τ value of the mixed isotopic species. This value can also be represented in terms of α, from classical isotopic exchange kinetic analysis, where α represents the fraction of heavy atoms in the gas phase in a

particular molecule.

$$\alpha(N_2) = \frac{[^{15}N_2] + 0.5[^{15}N^{14}N]}{[^{15}N_2] + [^{14}N^{15}N] + [^{14}N_2]} \quad [1]$$

In this case $[N_iN_{2-i}]$ represents the mole fraction (or concentration) of the corresponding molecule. Thus the α function represents the breakthrough function of ^{15}N atoms into specific product molecules. The τ value can thus be calculated using either of the following formulae;

$$\tau_{(\text{total})} = \tau_{(\text{unlabelled})} + 0.5 * (\tau_{(\text{mixed labelled})}) = \int_0^\infty \tilde{\alpha}\, dt, \quad [2]$$

where $\tilde{\alpha}$ represents $(1-\alpha)$ in the case of the ^{14}NO to ^{15}NO switch and α in the case of the ^{15}NO to ^{14}NO switch.

In the present case the individual τ values are presented as distinct from the α function as the latter, while providing valuable mechanistic insights in conjunction with mathematical modelling, loses the information regarding the percentage of the product molecules formed which are of mixed isotopic labels. Both methods obviously yield the same values for $\tau_{(\text{total})}$—the mean surface lifetime for the intermediate species leading to reaction products. It should be noted that an error associated with the calculation of each τ value is ca. 0.5 s.

Table 1 shows how the mean surface residence times (τ) for N_2 and N_2O precursors change as a function of the reaction temperature over samples of 1% Pt–SiO_2. We can see that there is little difference between the mean surface residence times for N_2 and N_2O precursors as the temperature is changed between 225 and 247°C. Further increase in the temperature to 263°C results in a measurable decrease in the average surface residence time of N_2, while having little influence on the N_2O value.

These values can be used, in conjunction with the rate of formation of the product species (N_2 or N_2O), to give a total value for the number of adsorbed species on the surface under given reaction conditions leading to the product (N_{ads}) (17).

$$2 * \tau_{(\text{total})} * r_{(N_2 \text{ or } N_2O)} = N_{(N_2 \text{ or } N_2O)} \quad [3]$$

In the more general situation, for a reaction as detailed below,

$$\sum v_i A_j + \sum v'_{i_u} A'_{i_u} \Leftrightarrow \sum v_j B_j + \sum v'_{j_u} B'_{j_u},$$

(where A_i represents a labelled reactant, B_j represents a labelled product, v is a stoichiometric coefficient, and the prime mark, along with the subscript u designates unlabelled species), the following equation can be used, in the case of an A + ( ) → A + ( ) switch, to calculate surface concentrations:

$$\sum_{i=1}^{R} n_{Ai} V \cdot C_{Ai}^{\text{out}} \int_0^\infty \tilde{\alpha}_{Ai}\, dt + \sum_{j=1}^{P} n_{Bj} \cdot V \cdot C_{Bj}^{\text{out}} \int_0^\infty \tilde{\alpha}_{Bj}\, dt = m_{\text{cat}} \cdot \sum_{k=1}^{S} \Theta_k \tilde{\alpha}^0_{\Theta_k} = m_{\text{cat}} \cdot N_{\text{Tot}} \tilde{\alpha}^0_{\Theta}. \quad [4]$$

Here P, R, S represent the number of products, reactants, and surface species. A_i are the labelled reactants, $i = 1, \ldots, R$; B_j are labelled product molecules, $j = 1, \ldots, P$; V is the total flow rate [l/s], n_{Ai}, n_{Bj} the number of atoms of a labelled element per molecule (e.g., for N_2, $n_{N_2} = 2$), C_{Ai}^{out}, C_{Bj}^{out} the concentration of labelled reactants and products exiting the reactor [mol/l]; $\tilde{\alpha} = (1 - \alpha_{A(B)})$ for the forward switch and $(\alpha_{(A)B})$ for the reverse switch; $\tilde{\alpha}^0_{\Theta_k}$ is the initial fraction of the corresponding isotope in the surface intermediate k, $k = 1, \ldots, S$). This fraction will normally be the same for all intermediates from $k = 1, \ldots, S$, at the time of switching $\tilde{\alpha}^0_{\Theta_k} = \tilde{\alpha}^0_{\Theta}$ and $\tilde{\alpha}^0_{\Theta}$ is 1 in the case where a labelled molecule fully replaces an unlabelled one; m_{cat} = mass of catalyst in g; Θ_k = concentration of labelled surface intermediate k, $k = 1, \ldots, S$ [mol of atoms/g] and N_{tot} represents the average total concentration of surface intermediates [mol atom/g]. This equation can allow the calculation of the concentration of all the NO-derived surface species on the catalyst under reaction conditions. The calculation of integrals must allow for the gas phase hold up of the system, i.e., the Ar trace must be allowed for.

In our case, for a forward switch $^{14}NO + C_3H_6 + O_2 \rightarrow {}^{15}NO + C_3H_6 + O_2$ this equation can be written as

$$V \cdot \left(C_{NO}^{\text{out}} + C_{NO_2}^{\text{out}}\right) \int_0^\infty (1 - \alpha_{NO})\, dt + 2 \cdot V \cdot C_{N_2}^{\text{out}} \int_0^\infty \left(1 - \alpha_{N_2}\right) dt + 2 \cdot V \cdot C_{N_2O}^{\text{out}} \int_0^\infty \left(1 - \alpha_{N_2O}\right) dt = m_{\text{cat}} \cdot N_{\text{Tot}}. \quad [5]$$

These properties (τ, N_{ads}, and N_{tot}—the mean surface residence time, the concentration of adsorption sites leading to product, and the total number of adsorption sites) are standard values derivable from any SSITK analysis and are not dependent on any proposed mechanism of reaction (17).

The values determined for the current reaction are detailed in Table 2. There it can be seen that while the mean surface residence time remains relatively unchanged as the temperature is raised from 225 to 247°C the total number of

TABLE 1

τ Values (Mean Surface Residence Times (s) of Species Leading to Specific Product Molecules) Calculated from the Observed Normalised Profiles Following Eq. [2]

T/°C	τNN s	$\tau N^{15}N$ s	τNNO s	$\tau N^{15}NO$ s	$\tau_{(\text{tot})}(N_2)$	$\tau_{(\text{tot})}(N_2O)$	$\tau_{(\text{tot})}$ $(N_2 + N_2O)$
225	1.8	6.7	0	4.7	5.2	2.4	7.6
247	2.2	7.1	0	4.4	5.8	2.2	8.0
263	1.9	4.7	0	4.2	4.3	2.1	6.4

TABLE 2

τ Values, r, the Rate of Production of N_2 and N_2O in μmol g^{-1} s^{-1}, Determined from the Changes in the Mass Spectrometer Signals, and Resultant N Values in μmol g^{-1} (the Total Number of Surface Intermediates Leading to N_2 and N_2O Products) Derived from Eq. [3]

T/°C	$\tau_{(total)}$ N_2	$\tau_{(total)}$ N_2O	rN_2 μmol/gs	rN_2O μmol/gs	$N(N_2)$ μmol/g	$N(N_2O)$ μmol/g	N(tot) μmol/g
225	5.2	2.4	0.02	0.07	0.21	0.34	0.55
247	5.8	2.2	0.06	0.10	0.70	0.44	1.14
263	4.2	2.1	0.10	0.15	0.86	0.63	1.49
328	~0.1	~0.0	0.43	0.45	—	—	—

Note. Values for $N(N_2)$ and $N(N_2O)$ are not calculated for the final temperature as the τ values calculated are below the error limits of the experiment.

sites producing N_2 and N_2O is increased. This is one reason for the increased activity of the catalyst.

At higher temperatures (above the maximum in NO_x conversion) the mean surface residence times of the main product molecules (N_2 and N_2O) became almost impossible to determine due to their closeness to the Ar traces as well as the difficulties discussed above in the overlap of the $^{14}NO_2$ and $^{15}N_2O$ signals. These values are shown for completeness in the final row of Table 2, but they are not used to calculate any parameters regarding the surface concentrations of adsorbed intermediates.

Also, at these higher temperatures, as seen in Fig. 1, the residence time for NO increased dramatically relative to those seen at temperatures below the NO_x conversion maximum. This resulted in a τ value of 5.1 for NO at 328°C compared to values indistinguishable from the Ar trace at lower temperatures.

We can further relate these values with surface coverages of the Pt by calculating the number of surface species that go on to form N_2 and N_2O per unit Pt surface area. This analysis is presented in Table 3 for N_2 and N_2O. The 1% Pt–SiO_2 sample has a dispersion of 0.22 which is equivalent to having a surface Pt concentration of about 11.2 μmol g^{-1} catalyst. Table 4 shows a similar analysis for NO in which case it is seen that the Pt is covered in 64% of a monolayer

TABLE 3

The Fraction of Pt Surface (θ) Covered by Intermediates Which Lead to N_2 and N_2O under Reaction Conditions at Different Temperatures under $NO/C_3H_6/O_2$ Reaction Conditions

T/°C	$N(N_2)$	$N(N_2O)$	$Pt_{(s)}$/ μmol g^{-1}	$\theta(N_2)$ × 100	$\theta(N_2O)$ × 100	θ(tot) × 100
225	0.21	0.34	11.2	1.9	3.0	4.9
247	0.70	0.44	11.2	6.3	3.9	10.2
263	0.86	0.63	11.2	7.7	5.6	13.3

TABLE 4

Mean Surface Residence Times, Rates of Flow over the Catalyst, Concentration of Adsorption Sites, and Pt Surface Coverage for NO over 1% Pt–SiO_2 in the $NO/C_3H_6/O_2$ Reaction as a Function of Temperature

T/°C	τ(NO)/s	r NO μmol g^{-1} s^{-1}	N (NO) μmol g^{-1}	θ NO × 100	θ N total × 100
225	~0	12.0	~0	~0	4.9
247	~0	11.8	~0	~0	10.2
263	~0	11.3	~0	~0	13.3
328	5.1	1.36	7.2	64.5	64.5

of NO at 328°C. It must be remembered in this final case that the catalyst is not acting differentially.

Another important dynamic feature of the products is the dependence of the fraction of heavy isotope (^{15}N in our case) in the gaseous phase upon time ($\alpha(t)$). Transient curves for $\alpha(N_2)$ and $\alpha(N_2O)$ after the $^{14}NO/C_3H_6/O_2 \rightarrow {}^{15}NO/C_3H_6/O_2$ switch at 225°C are shown in Fig. 3. It is quite noticeable that $\alpha(N_2O)$ rises more sharply than $\alpha(N_2)$. This indicates that N_2O is isotopically the first product and that N_2 is isotopically second (see Discussion). This is another

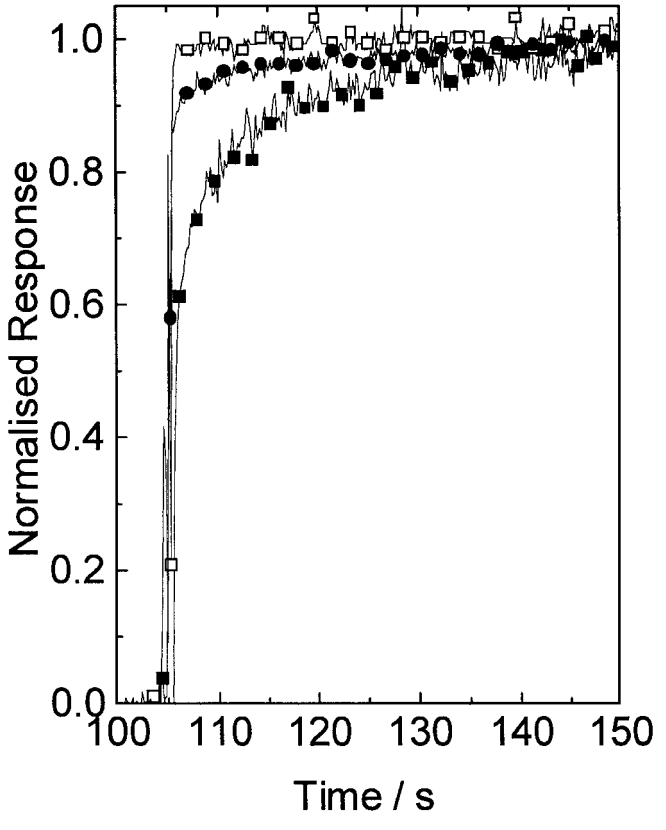

FIG. 3. $\alpha(N_2)$ and $\alpha(N_2O)$ as a function of time following a $^{14}NO \rightarrow {}^{15}NO$ switch over 1% Pt–SiO_2 at 225°C; Inverted Ar (□), $\alpha(N_2)$ (■), $\alpha(N_2O)$ (●).

indication that the residence time of surface intermediates leading to N_2O is less than the residence time for intermediates leading to N_2 and is seen in all cases where ^{14}NO is replaced by ^{15}NO in the reactant stream.

DISCUSSION

A number of important points can be derived from the SSITK analysis. First, within the limits of the system, no NO desorption processes can be discerned below the temperature of the maximum NO_x conversion. This is a significant result as it indicates that all the NO which adsorbs on the catalyst goes on to produce either N_2 or N_2O. It must be remembered however, that at these lower temperatures there is a relatively large amount of NO in the gas phase and therefore even the slightest difference between the Ar trace and the $^{14}NO/^{15}NO$ traces would be indicative of a very large surface concentration of NO coupled to a fast desorption process. However, we detected no such difference between the Ar and $^{14}NO/^{15}NO$ traces.

Another important point is that the mean surface residence time for NO goes from zero at low temperatures to a rather large value (5.31 s) at high temperatures. This is unusual in a catalytic reaction since the response of a surface species to an increase in temperature should be a decrease in the mean surface residence time. The observed increase in residence time can be explained by considering the difference in the chemical nature of the Pt surface at low and high temperatures. At low temperatures, where there is unreacted C_3H_6 in the exhaust gas, we have shown ((7, 8) Part 1 (29)) that the Pt surface is reduced and covered in carbonaceous species. There are thus very few adsorption sites available for NO which would allow an adsorption/desorption process to be established. In contrast, at high temperatures, where all the C_3H_6 is consumed, the Pt surface is oxidised and there are sites available which allow a steady-state NO adsorption/desorption process to be set up, quite probably involving $NO_{2\ ads}$-type species.

This can be envisaged to take place through an $NO_{(g)} + Pt\text{-}O \Leftrightarrow Pt\text{-}NO_{2\ ads}$ interaction on the oxidised Pt surface. Thus, the reason for the increased surface residence time as the temperature is raised is that we have two fundamentally different surfaces depending on the temperature and the high temperature (oxidised) surface is much more capable of adsorbing NO.

There is little difference between the surface residence times for N_2 and N_2O precursors as the temperature is raised from 225 to 247°C. However, further increases in the temperature result in a discernable decrease in the residence time for N_2 precursors while not having a serious effect on the τ value for the N_2O precursors. It is obvious that the N_2 precursors on the surface have a longer mean surface lifetime than the N_2O precursors. This indicates that the N_2O precursors are more reactive on the catalyst surface than the N_2 precursors. The inverse of the mean surface residence time can serve generally as an indicator of the "reactivity" of the surface species, i.e., the longer the intermediates stay on the surface the less reactive are the sites upon which they reside.

The rate of production of N_2 and N_2O increases with temperature. This is due, in the case of N_2 formation, both to an increase in the number of sites as well as to an increase in the reactivity of sites leading to N_2 formation, as seen in Table 2. The reactivity of sites leading to N_2O formation is generally unchanged by the increase in temperature from 225 to 263°C but the number of sites available increases by a factor of 2.

The concentration of sites responsible for making N_2/N_2O increases with temperature between 225 and 263°C. In terms of the previously proposed mechanism (7) this could be explained by the increased action of O_2 in removing carbonaceous deposits from the Pt as the temperature is raised and thus freeing up sites for NO adsorption and thus N_2/N_2O formation. The reason for the enhanced activity of the sites generating N_2 could be explained by an increased propensity for NO dissociation at the higher temperatures.

The relative responses of the N_2O and N_2 unlabelled product molecules following the $^{14}NO \rightarrow {}^{15}NO$ switch might also give some information regarding the proposed mechanism of the reaction. $^{14}N_2$ continues to be produced while it is seen that $^{14}N_2O$ is no longer formed once the ^{14}NO is removed. In terms of the previously proposed mechanism, $^{14}N_2$ is formed from the interaction of two $^{14}N_{ads}$ species on the surface while $^{14}N_2O$ is formed from the interaction of an $^{14}N_{ads}$ with a $^{14}NO_{ads}$. It now appears that this formation of $^{14}N_2O$ is considerably faster than that of $^{14}N_2$ on the catalyst surface. This could be explained by postulating a pool of $^{14}NO_{ads}$ intermediates, which go on to form $^{14}N_2O$ through interaction with a $^{14}N_{ads}$ species. The $^{14}NO_{ads}$ need only be present in a very low concentration but be in rapid equilibrium with gas phase NO. This NO_{ads} species does not dissociate. It simply acts to trap the $^{14}N_{ads}$ species which is then removed from the catalyst as $^{14}N_2O$. This is in line with the previously proposed mechanism. However, a more detailed analysis of the SSITKA profiles would be needed to fully confirm the operation of this mechanism.

We have also considered the possibility of an interaction between gas phase ^{14}NO and adsorbed ^{14}N yielding gas phase $^{14}N_2O$ (Eley–Rideal mechanism). However, if this was the case then, after the switch, we would expect the mixed labelled N_2O to be far more prevalent than the mixed-labelled N_2. This would be expected because, in order to form the mixed-labelled N_2, the ^{15}NO has to adsorb and dissociate before it can combine with a ^{14}N atom and desorb. While the production of mixed-labelled N_2O is high, it is not high enough to suggest an Eley–Rideal mechanism. Also the production of mixed-labelled N_2 continues after

production of mixed-labelled N_2O ceases. Another possible explanation might be that there are sites on the surface which can produce N_2 but are unable to produce N_2O and that it is from these sites that the mixed N_2 product is formed.

Another surprising point to note is the relatively large delay seen in the $^{14}N_2$ response relative to Ar. This, and the fact that ^{14}N labels are still being seen up to 120 s after the ^{14}NO is removed, indicates that the N_{ads} species on the surface might be relatively stable. This might in turn indicate that the rate determining process for the formation of N_2 under these conditions is not the adsorption and dissociation of NO, but rather the combination and desorption of 2 N atoms as N_2. This has been claimed for NO decomposition/reduction over Pd-supported catalysts (31).

The rapid formation of N_2O relative to N_2 under our experimental conditions does not auger well for the development of Pt-based lean-deNO_x catalysts for the selective reduction to of NO to N_2 rather than to N_2O. For this to happen the rate of dissociation of NO on the surface would have to be faster than the rates of reaction of NO with N_{ads} to form N_2O. This is obviously not the case with these Pt-based systems.

It can be seen from the low temperature data in Table 3 that at no time is more than 15% of the Pt surface given over to the production of N_2 or N_2O. This fits well with the data in the previous paper where it was seen that at these temperatures the Pt is practically covered by carbon. It is not surprising, therefore, that there are so few N_2/N_2O precursors on the surface. At high temperatures, the Pt is over 65% covered with NO_{ads} species. This is because the NO molecule is able to adsorb on PtO_x (as an $NO_{2\ ads}$ or an $NO_{3\ ads}$-type species).

"Isotopically First" Product Molecules

An important feature for the establishment of the mechanism of a catalytic reaction is the order of appearance of products from the reaction network. It is useful in these situations to establish which product is isotopically first. By the "isotopically first" product we mean the product which has the lowest residence time on the catalyst relative to all the other reaction products. If we consider a reactant $A_{(g)}$ and two products $B_{1(g)}$ and $B_{2(g)}$, then generally after an isotopic switch the fraction of heavy atoms in the gas phase of the isotopically first molecule (B_1) will be higher than that for the isotopically second (or last) molecule at all times, i.e., $\alpha(B_1) > \alpha(B_2)$. This is represented graphically in Fig. 3 where it is seen that $\alpha(N_2O) > \alpha(N_2)$, i.e., that the area between the $\alpha(N_2O)$ profile and the Ar profile is less than the area between the $\alpha(N_2)$ profile and the Ar profile.

This can be displayed in either of the proposed linear networked reaction schemes presented below where A is the reactant and B_1 and B_2 represent the isotopically first and isotopically second product molecules, respectively.

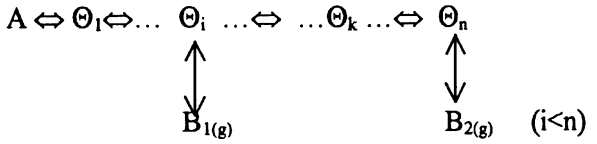

SCHEME 1

Or, in the more complex case,

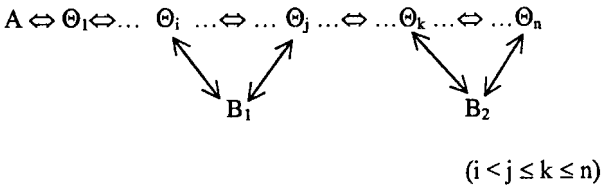

SCHEME 2

In these cases the production of the last product, B_2, normally involves the terminal (nth) intermediate. More complex cases where B_2 might be produced from intermediates with $k < i$ and $j > k$ are not discussed here and will be discussed in a subsequent publication (30).

"Isotopically final" molecules might also be produced by readsorption of the B_1 molecule followed by its transformation on the surface to form the B_2 molecule. In our case this would involve the readsorption of N_2O from the gas phase and its decomposition/reduction on another site to form the N_2 molecule (Scheme 3).

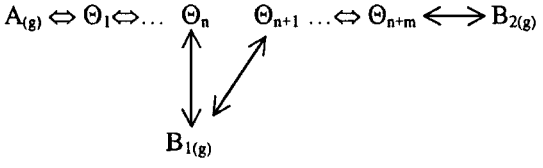

SCHEME 3

In the case of possible parallel paths (Scheme 4) the profiles $\alpha(B_1)$ and $\alpha(B_2)$ can intersect each other before steady state is reached. Also if parallel paths do exist and the two functions do not intersect then the isotopically first product will be the species with the smaller total residence time (τ_{rt}) of surface intermediates leading to its generation, as detailed in Eq. 6.

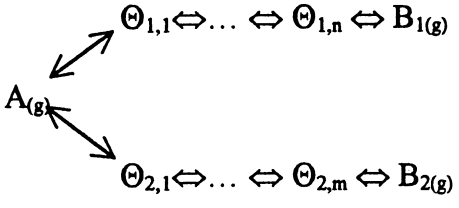

SCHEME 4

$$\tau_{(rt)(B_1)} = \int_0^\infty \left(1-\alpha_{(B_1)}\right) dt. \quad <\tau_{(rt)(B_2)} = \int_0^\infty \left(1-\alpha_{(B_2)}\right) dt. \qquad [6]$$

Additional difficulties may arise in the interpretation of experimental data with respect to the order of isotopically labelled products. These become important in situations where homo- and hetero-exchange of the product molecules with the surface species adsorbed on the catalyst takes place. These will be fully discussed in a subsequent publication (30).

In the present case the probability of either the parallel network or the network involving readsorption of N_2O providing a mechanism for the current reaction is quite small. The reasons for this exceed the scope of the present work but will be dealt with elsewhere (30).

All the experiments we have carried out have consistently shown that, regarding the $\alpha(t)$ functions, N_2O is always the isotopically first product. In terms of the reaction mechanism this means that N_2O must be produced from surface intermediates formed earlier, whereas N_2 is formed from later intermediates.

In our present case the observed difference between the $\alpha(N_2O)_t$ and $\alpha(N_2)_t$ profiles might also indicate the presence of *intermediate* pool(s) of relatively large concentration. These would be represented by the pool(s) between Θ_j and Θ_n in the case of a linear network, as indicated in Schemes 1 and 2.

Another reason for this might be that the production of N_2O follows the interaction between earlier precursors whereas the production of N_2 takes place exclusively through terminal precursors, e.g., as shown in the special Scheme 5.

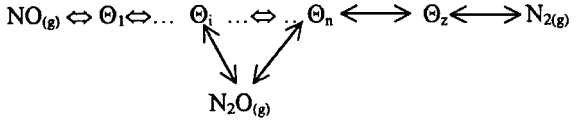

SCHEME 5

This result differs from that of Ozkan *et al.* (25) in their study of the NO/CH_4/O_2 reaction over Pd–TiO_2 catalysts. These authors noted the release of isotopically labelled N_2 first from the catalyst and second, over a far longer period of time, the release of isotopically labelled N_2O. However, this may simply indicate that the mechanism of N_2 and N_2O formation is different on Pt and Pd.

CONCLUSIONS

The main points which come from this SSITK analysis are as follows:

- There is, within the experimental limits, no discernible steady state $NO_{(g)} \Leftrightarrow NO_{ads}$ equilibrium onto the Pt surface at low temperatures where there is excess C_3H_6 in the exhaust stream from the catalytic reactor during the NO/C_3H_6/O_2 reaction. This is in contrast to what is found at higher temperatures where NO_2 is a major product. This can be ascribed to the fact that at high temperatures the Pt surface is oxidised. NO can adsorb onto and desorb from these Pt-O_{ads} species whereas NO does not adsorb readily on the carbon-covered (reduced) Pt surface.
- There are N_2 and N_2O precursors on the surface of the catalyst for measurable times during the reaction. The mean surface residence times for the N_2 precursors decreases as the temperature increases between 247 and 263°C.
- The measured concentrations of sites for both N_2 and N_2O production increase with temperature. This increase is twofold for N_2O production and fourfold for N_2 production over the temperature range from 225 to 263°C.
- The reaction rate increases seen with increasing temperature are solely due to an increase in the number of active sites in the case of the N_2O formation but are due to both an increase in the number of active sites and in their "reactivity" in the case of N_2 formation.
- N_2O is the isotopically first product while N_2 is the second. This indicates that there are additional precursors for N_2 production or that N_2O must be produced from surface intermediates formed earlier, whereas N_2 is formed from the later intermediates.
- The formation of N_2O is more rapid than that of N_2 and it is possible, but unlikely, that it is formed through an Eley–Rideal-type mechanism where gaseous NO interacts with adsorbed N atoms.

The formation of N_2O as the isotopically first product is in line with what would be expected from the previously proposed reaction mechanism (7). Changes in the selectivity to N_2O, which have previously been ascribed to an increase in the NO dissociation activity, have been seen to be attributable to an increase in the "reactivity" of sites leading to N_2 relative to sites leading to N_2O. Both of these results are in qualitative agreement with the previously proposed mechanism. Further work to both clarify the reaction mechanism and to generate quantitative values of such parameters as surface rates and the number and concentration of surface intermediates is in progress (30).

ACKNOWLEDGMENTS

We are grateful to the EPSRC for supporting this research through Contract GR/K70403. AAS thanks NATO and The Royal Society for providing a Fellowship (NATO/96A).

REFERENCES

1. Burch, R., Ed., *Catal. Today* **26** (1995).
2. Iwamoto, M., Ed., *Catal. Today* **22** (1994).
3. Burch, R., and Scire, S., *Appl. Catal. B* **3**, 295 (1994).
4. Sullivan, J. A., and Cunningham, J., *Appl. Catal. B* **15**, 275 (1998).

5. Iwamoto, M., and Mizuno, N., *J. Automobile Eng.* **207**, 23 (1993).
6. Ansell, G. P., Golunski, S. E., Hayes, J. W., Burch, R., and Millington, P. J., *Stud. Surf. Sci. Catal.* **96**, 577 (1995).
7. Burch, R., and Watling, T. C., *Catal. Lett.* **43**, No. 1–2, 19 (1997).
8. Burch, R., and Watling, T. C., *J. Catal.* **169**, 45 (1997).
9. Captain, D. K., Robberts, K. L., and Amaridis, M. D., *Catal. Today* **42**, 93 (1998).
10. Sasaki, M., Hamada, H., Kintaichi, Y., Ito, Y., and Tabata, M., *Catal. Lett.* **15**, 297 (1992).
11. Burch, R., and Ottery, D., *Appl. Catal. B* **9**, L19 (1996).
12. Burch, R., and Watling, T. C., *Appl. Catal. B* **17**, No. 1–2, 131 (1998).
13. Burch, R., Fornasiero, P., and Southward, B. W. L., *J. Chem. Soc. Chem. Comm.* 625 (1998).
14. Burch, R., Fornasiero, P., and Watling, T. C., *J. Catal.* **176**, 204 (1998).
15. Happel, J., "Isotopic Assessment of Heterogeneous Catalysts," Academic Press, Orlando, FL, 1986.
16. Happel, J., Walter, E., and Lecourtier, Y., *J. Catal.* **123**, 12 (1990).
17. Shannon, S. L., and Goodwin, J. G., *Chem Rev.* **95**, 677 (1995).
18. Hanssen, K. F., Blekkan, E. A., Schanke, D., and Holmen, A., *Stud. Surf. Sci. Catal.* **109**, 193 (1997).
19. Bajusz, I. G., Kwik, D. J., and Goodwin, J. G., *Catal. Lett.* **48**, No. 3–4, 151 (1997).
20. Efstathiou, A. M., and Verykios, X. E., *Appl. Catal. A* **151**, No. 1, 109 (1997).
21. Ali, S. H., and Goodwin, J. G., *J. Catal.* **170**, No. 2, 265 (1997).
22. Oukaci, R., Blackmond, D. G., Goodwin, J. G., Jr., and Gallagher, G. R., *in* "Catalytic Control of Air Pollution," Ch. 5, pp. 61–72. American Chemical Society, Washington, DC, 1992.
23. Efstathiou, A. M., and Fliatoura, K., *Appl. Catal. B* **6**, No. 1, 35 (1995).
24. Janssen, F. J. J. G., Van Den Kerkhof, F. M. G., Bosch, H., and Ross, J. R. H., *J. Phys. Chem.* **91**, No. 27, 6633 (1987).
25. Janssen, F. J. J. G., Van Den Kerkhof, F. M. G, Bosch, H., and Ross, J. R. H., *J. Phys. Chem.* **91**, No. 23, 5921 (1987).
26. Kumthekar, M. W., and Ozkan, U. S., *Appl. Catal. A* **151**, No. 1, 289 (1997).
27. Kumthekar, M. W., and Ozkan, U. S., *J. Catal.* **171**, 54 (1997).
28. Burch, R., Halpin, E., and Sullivan, J. A., *Appl. Catal. B* **17**, No. 1–2, 115 (1998).
29. Burch, R., and Sullivan, J. A., *J. Catal.* **182**, 489 (1999).
30. Burch, R., Shestov, A. A., and Sullivan, J. A., in preparation.
31. Bowker, M., Personal communication.